Japanese Journal of
Applied Physics

REGULAR PAPER • OPEN ACCESS

Enhanced photoluminescence intensity of buried InGaAs/GaAs(001) quantum wells by sulfur termination

To cite this article: Zhao Ma *et al* 2024 *Jpn. J. Appl. Phys.* **63** 121002

OPEN ACCESS

Japanese Journal of Applied Physics **63**, 121002 (2024) **REGULAR PAPER**

https://doi.org/10.35848/1347-4065/ad9802

Enhanced photoluminescence intensity of buried InGaAs/GaAs(001) quantum wells by sulfur termination

Zhao Ma[1,2*], Takaaki Mano[1*], Akihiro Ohtake[1], and Takashi Kuroda[1,2]

[1]National Institute for Materials Science, Tsukuba, Ibaraki 305-0044, Japan
[2]Department of Applied Chemistry, Graduate School of Engineering, Kyushu University, Fukuoka 819-0395, Japan

*E-mail: MA.Zhao@nims.go.jp and MANO.Takaaki@nims.go.jp

Received September 12, 2024; revised November 25, 2024; accepted November 26, 2024; published online December 16, 2024

Sulfur (S) termination of III–V semiconductor surfaces is an effective technique for passivating surfaces to prevent oxidation. In this study, we systematically investigated the effects of S termination by $(NH_4)_2S_x$ treatment on enhancement of the photoluminescence (PL) properties of buried InGaAs/GaAs(001) quantum wells (QWs). X-ray photoelectron spectroscopy (XPS) and PL measurements revealed that the $(NH_4)_2S_x$ treatment suppresses the formation of surface oxides, especially arsenic oxides, and enhances the PL intensity of QWs. Clear correlation between the PL and XPS results suggests that greater PL intensity is attributable to a reduction in the number of nonradiative recombination centers at the surface caused by arsenic oxide formation. In addition, from the observed temporal changes in PL intensities, we found that the S-terminated surfaces exhibit long-term and high resistance to surface oxidation by air exposure.

1. Introduction

III–V semiconductor-based heterostructures are widely used in the field of high-performance optoelectronic devices, including high-electron mobility transistors,[1,2] heterojunction bipolar transistors,[3,4] laser and light-emitting diodes, photodetectors, and solar cells.[5] During the crystal growth or etching processes of these heterostructures, their surfaces are kept more or less clean, with only small amounts of attached foreign atoms. When the structures are exposed to ambient air after processing, the surfaces come into contact with oxygen and other foreign contaminants. The surfaces of GaAs-based structures are then gradually oxidized, with a high density of surface states being formed on these surfaces, resulting in strong Fermi-level pinning effects near the midgap of GaAs.[6,7] Around 1990, various surface-termination processes using VI-group element atoms, such as sulfur (S) and selenium (Se), were actively investigated with the aim of suppressing these surface oxidation processes, chiefly to improve the devices' Schottky and other properties for use in metal-insulator-semiconductor devices.[7–9] To form terminated surfaces, wet processes using $Na_2S{\cdot}9H_2O$,[10,11] $(NH_4)_2S$,[12–14] $(NH_4)_2S_x$,[7,8,15–17] Na_2Se in NH_4OH,[9] $(NH_4)_2S + Se$,[18] and vacuum deposition of elemental sulfur[19,20] or selenium[21–31] in ultra-high vacuum (UHV) chambers were attempted, demonstrating their effectiveness and potential for practical application.

Surface-termination techniques for passivating semiconductor nanostructures such as nanowires, nanopillars, and quantum dots are increasingly coming back into the limelight.[32–35] In these nanostructures, the core regions are often exposed to air and/or located very close to the surface. The oxidized surfaces therefore act as nonradiative-recombination centers and/or charge trapping sites that degrade the optical properties of the nanostructures by decreasing the optical emission intensity[10] and/or broadening the optical emission linewidth.[32–35] Suppression of surface oxidation is therefore a critical challenge for improving the optical properties of these nanostructures. In more recent studies, sulfur termination followed by coating with a dielectric material such as Al_2O_3 or SiO_x are often used for surface passivation.[35–38] Enhanced photoluminescence (PL) emission and narrowing of the single quantum dot spectra have been reported. However, the effects of S termination on the optical properties have not yet been elucidated. For the further improvement of the optical properties of nanostructures by using surface termination techniques, it is necessary to understand in greater detail the surface-termination effects on surface oxidation and their impact on optical properties.

In this study, we systematically investigated the impact of an $(NH_4)_2S_x$-based passivation process on the optical properties of buried quantum wells (QWs) and the chemical composition of the GaAs (001) surfaces by means of PL spectroscopy and X-ray photoelectron spectroscopy (XPS) measurements. The inhibitory effects of S termination on surface oxidation were clearly shown. Suppressing surface oxidation clearly enhanced PL intensity.

2. Experimental methods

Our experimental procedures are shown schematically in Fig. 1. As starting material, we used an identical single InGaAs QW structure grown on GaAs (001) substrate using molecular beam epitaxy. After growth of a 300 nm GaAs buffer layer at 580 °C, 10 nm $In_{0.12}Ga_{0.88}As$ QW was grown at 490 °C. The QW was then capped with 100 nm GaAs at 490 °C. The surface was finally capped with amorphous As by supplying As_2 flux (1×10^{-5} Torr beam equivalent pressure) at room temperature for 30 min to protect the sample from oxidation after exposure to ambient air. Before performing each PL and XPS measurement the amorphous As was removed by dipping the samples in ~30% H_2O_2 solution. This procedure enabled us to study identical surfaces for each experiment. This sample is referred to as the "*Reference*" sample in this paper. It should be noted that the H_2O_2 solution oxidizes the GaAs surface. To remove the surface oxides, we immersed the samples in buffered potassium hydroxide (KOH) solution for 1 min,[17] followed by rinsing in ultra-pure water and N_2 gas blowing. The sample at this step is referred to "KOH-*treated*". For sulfur termination, the KOH-*treated* sample was dipped in ammonium sulfide solution with excess sulfur $[(NH_4)_2S_x]$ at 60 °C for 15 min. The sample was then taken out from the solution and dried by N_2 blow without

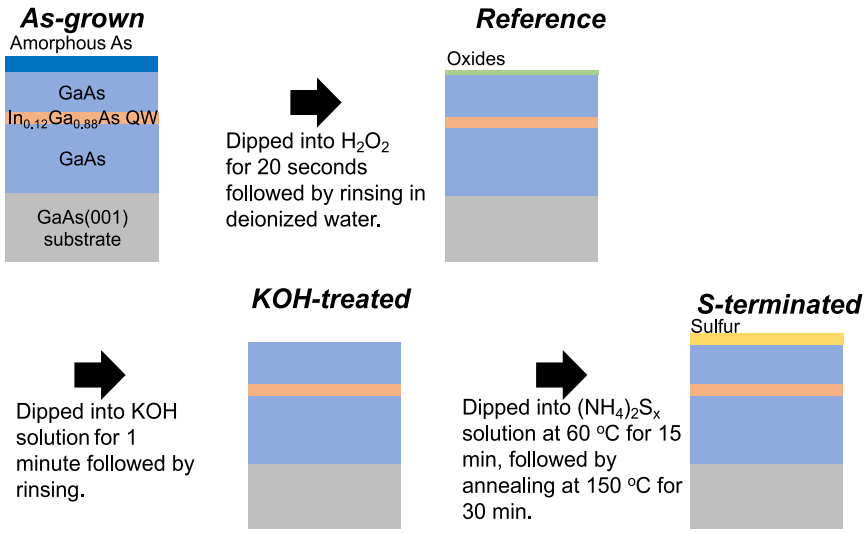

Fig. 1. Schematic drawing of experimental procedures.

rinsing in water. Finally, we annealed the sample in vacuum chamber at 150 °C for 30 min using a ramp heater to evaporate the excess sulfur atoms on the surface. The heating rate was 10 °C min^{-1}. The annealing temperature was carefully calibrated by using thermo-couples set at the sample position. The background pressure during the annealing was around 1×10^{-3} Pa. The sample at this step is referred to "*S-terminated*".

After each chemical treatment, the samples were stored in vacuum chamber to avoid further oxidation. To investigate the temporal change of PL and XPS signals with air exposure time, we took the samples out of the vacuum chamber and exposed them to the air for different periods from less than 30 min to 30 d. For the PL measurement, we used an Nd:YVO_4 based laser emitting at a wavelength of 532 nm. The PL signals were fed into a 50 cm spectrometer and detected by a cooled charge-coupled device camera. The PL measurement was performed mostly at 4 K, where the carrier thermal escape from the QW was efficiently suppressed. In addition, we measured the PL spectra at room temperature for the samples after long-term air exposure (7 month) to clarify the thermal impact on nonradiative recombination.

The surface chemical conditions were analyzed using an XPS measurement system (Surface Science Instruments M-Probe). XPS measurements were performed using monochromatic Al $K\alpha$ radiation (1486.6 eV) at room temperature. Photoelectrons were detected at an angle of 35° from the surface. The As 3d and Ga 3d spectra were measured and fitted using a Voigt function with the ratio of Gaussian to Lorentzian components fixed at 2.5. Peak separations of 0.70 eV and 0.45 eV, respectively, were assumed for the 5/2 and 3/2 spin–orbit components of As 3d and Ga 3d.

3. Results and discussion

Figures 2(a)–2(c) show the low-temperature PL spectra of the *Reference*, KOH-*treated*, and S-*terminated* samples, immediately after the chemical treatment (air exposure time of less than 30 min). While all the samples exhibited a clear PL emission peak at around 900 nm from the InGaAs QWs, there were significant differences in their intensity. The integrated PL intensities of the KOH-*treated* and S-*terminated* samples were 1.2- and 1.4-fold larger than that of the *Reference* sample, respectively, as seen in Fig. 2(d). The results reveal that both the KOH treatment and S termination are effective for enhancing the PL emission efficiency. We attribute the enhanced PL intensity to the decreased number of nonradiative recombination centers at the surfaces.

Next, we investigated the time-dependent change in the PL intensity of these samples with exposure to air. Figure 3 shows the changes in the integrated PL intensity of the three samples after air exposure for certain periods of time. As expected, the PL intensity of the *Reference* sample, where the surface oxides had already been formed by dipping in the H_2O_2 solution, exhibits marginal change: even after 30 d, the intensity decreased by only ~10% from the initial value. On the other hand, the PL intensity of the KOH-*treated* sample changed rapidly: after 5 d, the intensity decreased by more than 20%, reaching nearly the same level as that of the *Reference* sample, suggesting that the surface chemical condition of the KOH-*treated* sample converges with that of the *Reference* sample due to oxidation. The PL intensity of the S-*terminated* sample also decreased by 16% in the first five days, then more slowly later. It is important here to note that the intensity of the S-*terminated* sample is always more than 20% higher than that of the other two samples, suggesting that the S termination is stable even after exposure to air for one month.

We also measured the PL spectra at room temperature for all the samples after long-term storage in air (7 months). Figures 4(a)–4(c) show the room temperature spectra of the three samples, together with their low temperature spectra measured at 4 K. The PL signals at room temperature are around three orders of magnitude weaker than those measured at 4 K due to the impact of carrier thermal escape from the shallow QW. Remarkably, the intensity contrast between the three samples is more significant at room temperature than 4 K. At room temperature, the S-*terminated* sample shows intensities twice as strong as the others. However, at 4 K, the S-*terminated* sample shows intensities around 1.2 times higher than the other samples, the signature of which is similar with what we observed in Figs. 2 and 3. We attribute the enhanced contrast to increased probability that carriers reach the surface before being recombined in the QW.

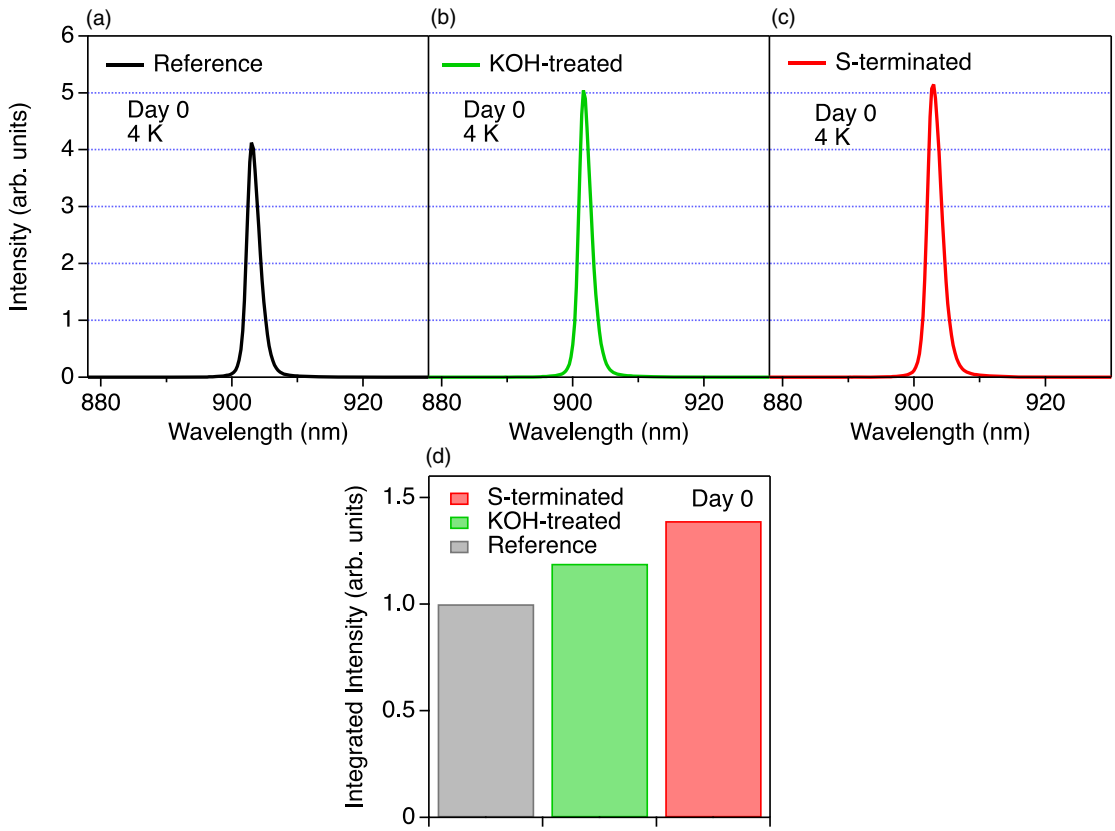

Fig. 2. Low-temperature PL spectra of (a) *Reference*, (b) KOH-*treated*, and (c) S-*terminated* samples right after the chemical treatment (Day 0). The integrated intensity of these spectra is plotted in (d).

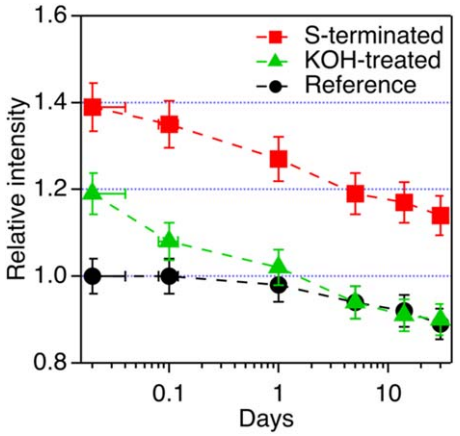

Fig. 3. Time-dependent change in the integrated PL intensity of the three samples after exposure to air for certain periods of time. They were measured at 4 K.

XPS measurements were carried out to study the chemical states of the three samples and their relation to their optical properties. Figures 5 and 6 respectively show the As 3d and Ga 3d core-level spectra. The spectra in (a) were measured from the sample within 30 min after the treatment, and those in (b) were measured from the sample that had been exposed to air for 14 d.

The As 3d spectra were fitted with components corresponding to Ga–As, AsO, As_2O_3, As_2O_5, and $GaAsO_4$, and the Ga 3d spectra were fitted with Ga–As, Ga_2O_3, and $GaAsO_4$ components. The quantities of Ga- and As-oxides measured from the *Reference* sample [top panels of Figs. 5(a) and 6(a)] are more than two-fold those measured on the cleaned (2×4)-reconstructed GaAs(001) surface after exposure to air for 24 h (data not shown). It is therefore confirmed that H_2O_2 treatment strongly facilitates the oxidation of the GaAs surface immediately after the removal of the amorphous-As cap layers. In the KOH-*treated* sample [middle panels of Figs. 5(a) and 6(a)], the oxide-related components are significantly lower than seen in the reference sample [Figs. 5(c) and 6(c)], indicating that the Ga- and As-oxides had been effectively removed by the KOH treatment.

When the *Reference* sample had been exposed to air for 14 d, the intensities of oxide-related components increased slightly [top panels of Figs. 5(a), 5(b) and 6(a), 6(b)]. On the other hand, for the KOH-*treated* sample, the oxide-related components had drastically increased after 14 d, such that their intensities were comparable with those of the *Reference* sample [middle panels of Figs. 5(a), 5(b) and 6(a), 6(b)]. This means that the KOH treatment was able to remove most of the oxides, but is not effective in suppressing oxide formation that takes place after long periods of exposure to air.

The As 3d spectrum measured immediately after the S treatment is shown in the bottom panel of Fig. 5(a). There is little evidence of components that would indicate the presence of As-oxides. While the formation of As-oxides is confirmed after 14 d, as shown in the bottom panel of Fig. 5(b), the amount of oxides is one order of magnitude smaller than those seen on the KOH-*treated* sample [Fig. 5(c)]. On the other hand, Ga-oxides components can

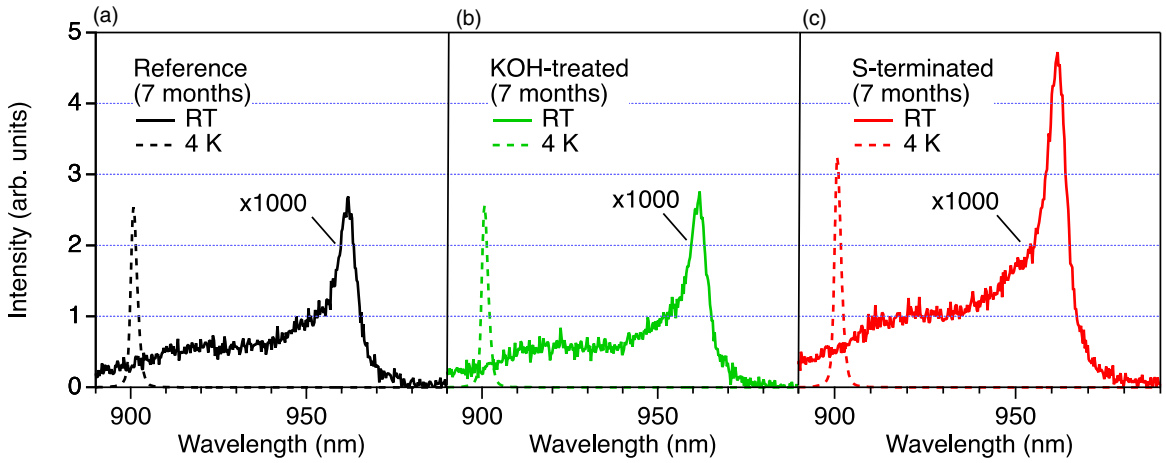

Fig. 4. PL spectra of the three samples after being stored in air for 7 months for the (a) *Reference*, (b) KOH-*treated*, and (c) S-*terminated* samples. The solid lines are the spectra measured at room temperature and the broken lines are the spectra measured at 4 K.

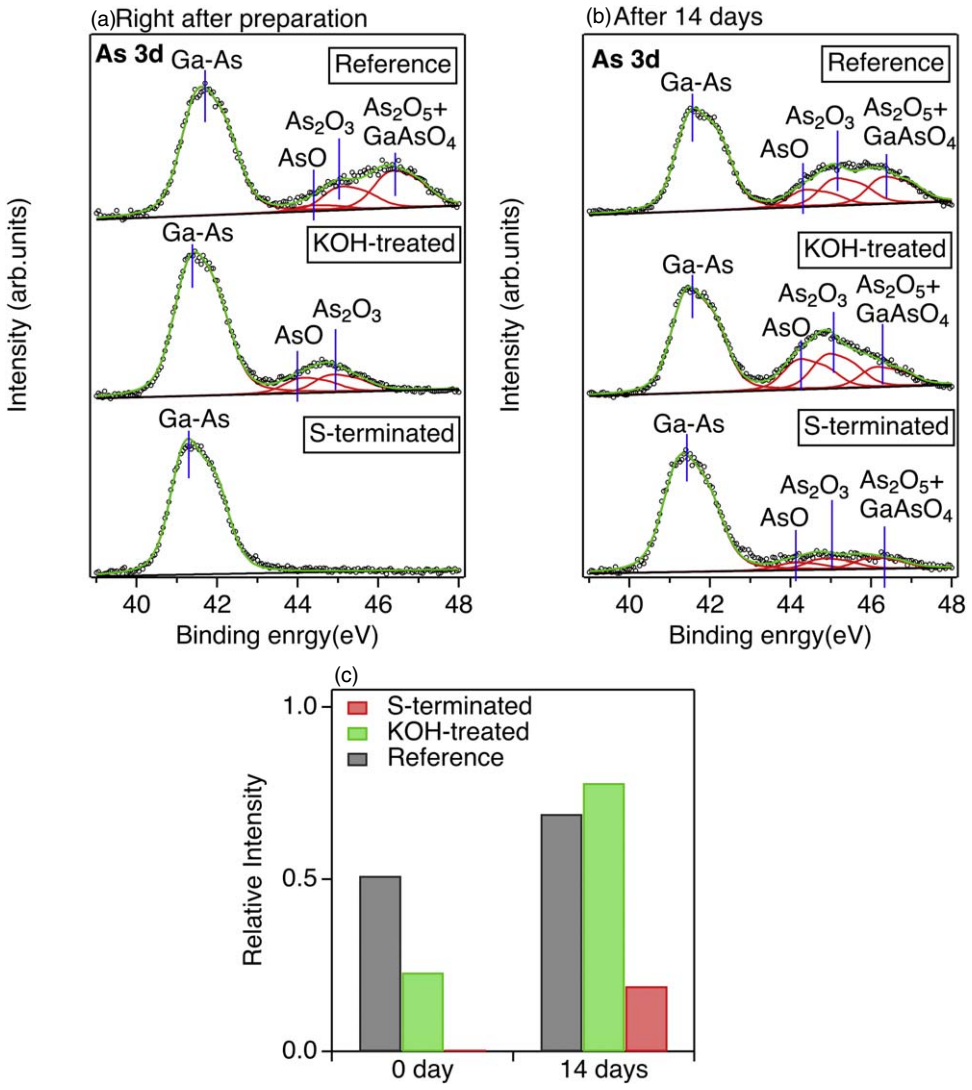

Fig. 5. As 3d core-level spectra of the three samples. (a) immediately after preparation and (b) after exposure to air for 14 d. The ratios of the oxide-related components (As–O/Ga–As) are plotted in (c).

be clearly seen in the spectrum measured immediately after the S treatment [bottom panel of Fig. 6(a)]; the quantities of Ga-oxides are much greater than those on the KOH-*treated* sample. However, the amount of Ga-oxides increased only minimally after 14 d, as shown in Fig. 6(c). The S treatment is therefore extremely effective in removing As-oxides, as well as in preventing further oxidation of both As and Ga.

A comparison of the the observed changes in the XPS spectra [Figs. 5(c) and 6(c)] with the PL results (Fig. 3),

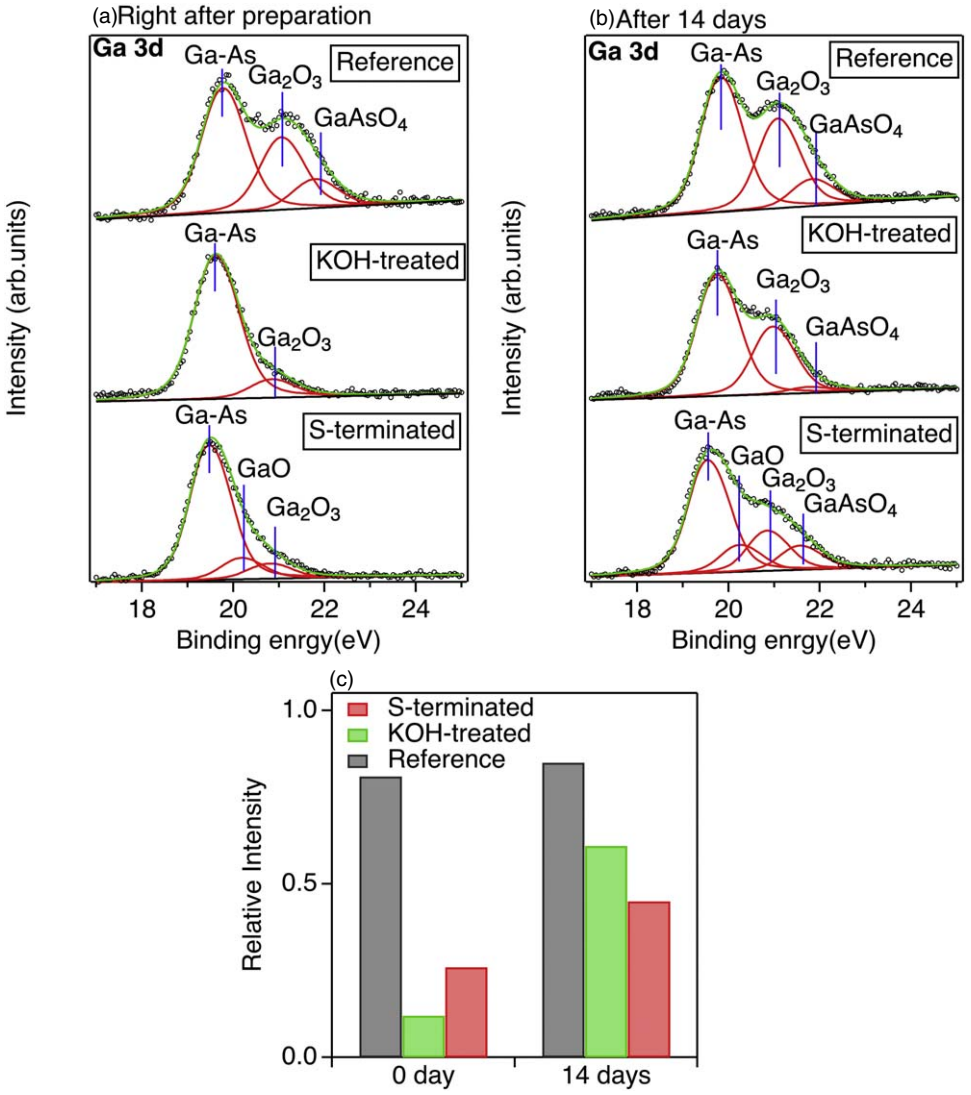

Fig. 6. Ga 3d core-level spectra of the three samples. (a) immediately after preparation and (b) after exposure to air for 14 d. The ratios of the oxide-related components (Ga–O/Ga–As) are plotted in (c).

reveals a clear correlation between them. Shown in Figs. 7(a), 7(b) are PL intensities plotted as a function of the XPS intensity ratio of As–O/Ga–As (Ga–O/Ga–As). The PL intensity monotonically decreases with increasing As–O/Ga–As ratio [Fig. 7(a)], while no clear correlation could be found for Ga-oxides [Fig. 7(b)]. It therefore appears that the formation of As-oxides increases the density of nonradiative recombination centers, resulting in the observed decrease in PL intensity.

It is important to note here that it is possible to maintain nearly As-oxide-free surfaces if the S-terminated samples are transferred to another vacuum deposition system within

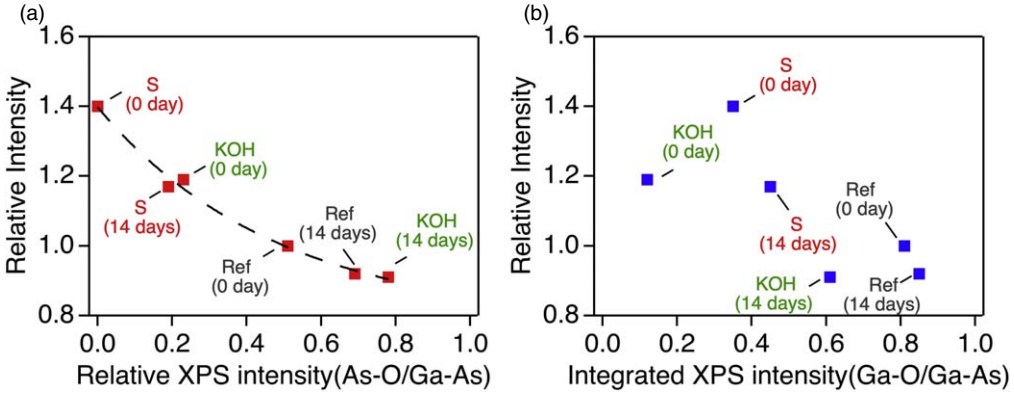

Fig. 7. PL intensities plotted as a function of the XPS intensity ratio of As–O/Ga–As (a) and Ga–O/Ga–As (b). Red dots represent data points. Broken line represents fitting of the experimental data.

30 min. By coating these surfaces with dielectric materials, the surface properties are likely to endure.[39] We have thus confirmed the effectiveness of S termination followed by coating with dielectric materials.

4. Conclusions

We studied the effects of sulfur termination using $(NH_4)_2S_x$ treatment on the photoluminescence properties of buried InGaAs QWs in GaAs (001). Immediately after S termination, we observed higher PL intensity than that seen in the H_2O_2-treated reference sample. After removing the surface oxides by KOH treatment, we observed an immediate enhancement. However, the PL intensity sharply decreases and falls to nearly the same level as that of the *Reference* sample after just a few days, since KOH treatment is not effective in suppressing oxide formation under conditions of long exposure to air. In contrast, the intensity of the S-*terminated* samples remained brighter than that of the *Reference* and KOH-*treated* samples even after 30 d. The surface chemical conditions as revealed by XPS showed the formation of As-oxides to be a major contributor to the nonradiative recombination process at the surface, since we observed a clear correlation between PL intensity and As–O/Ga–As ratio. S termination thus effectively and durably suppresses the formation of As-oxides at the surface.

Acknowledgments

This work was supported by the Innovative Science and Technology Initiative for Security, Grant No. JPJ004596, ATLA, Japan.

ORCID iDs

Zhao Ma https://orcid.org/0000-0003-0151-8592
Takaaki Mano https://orcid.org/0000-0002-6955-260X
Akihiro Ohtake https://orcid.org/0000-0002-3519-4613
Takashi Kuroda https://orcid.org/0000-0001-6445-7673

1) T. Mimura, S. Hiyamizu, T. Fujii, and K. Nanbu, "A new field-effect transistor with selectively doped GaAs/n-$Al_xGa_{1-x}As$ heterojunctions," Jpn. J. Appl. Phys. **19**, L225 (1980).
2) L. Pfeifer, K. W. West, H. L. Stormer, and K. W. Baldwin, "Electron mobilities exceeding 107 $cm^2 V^{-1} s^{-1}$ in modulation-doped GaAs," Appl. Phys. Lett. **55**, 1888 (1989).
3) P. M. Asbeck, M. C. F. Chang, J. A. Higgins, S. H. Sheng, G. J. Sullivan, and K. C. Wang, "GaAlAs/GaAs hetrojunction bipolar-transistors-issues and prospects for application," IEEE Trans. Electron Devices **36**, 2032 (1989).
4) K. Kurishima, H. Nakajima, T. Kobayashi, Y. Matsuoka, and T. Ishibashi, "Fabrication and characterization of high-performance InP/InGaAs double-heterojunction bipolar-transistors," IEEE Trans. Electron Devices **41**, 1319 (1994).
5) P. Bhattacharya, *Semiconductor Optoelectronic Devices* (Prentice Hall, Upper Saddle River, NJ, 1997) 2nd ed.
6) W. E. Spicer, P. W. Chye, P. R. Skeath, C. Y. Su, and I. Lindau, "New and unified model for schottky barrier and III–V insulator interface states formation," J. Vac. Sci. Technol. **16**, 1422 (1979).
7) H. Oigawa, J-F. Fan, Y. Nannichi, K. Ando, K. Sakai, and A. Koma, "Studies on and $(NH_4)_2S_x$-treated GaAs surface using AES, LEELS and RHEED," Jpn. J. Appl. Phys. **28**, L340 (1989).
8) H. Oigawa, J-F. Fan, Y. Nannichi, H. Sugahara, and M. Oshima, "Universal passivation effect on $(NH_4)_2S_x$ treatment on the surface of III–V compound semiconductors," Jpn. J. Appl. Phys. **30**, L322 (1991).
9) C. J. Sandroff, M. S. Hegde, L. A. Farrow, R. Bhat, J. P. Harbison, and C. C. Chang, "Enhanced electronic properties of GaAs surfaces chemically passivated by selenium reactions," J. Appl. Phys. **67**, 586 (1990).
10) C. J. Sandroff, R. N. Nottenburg, J-C. Bischoff, and R. Bhat, "Dramatic enhancement in the gain of a GaAs/AlGaAs heterostructure bipolar transistor by surface chemical passivation," Appl. Phys. Lett. **51**, 33 (1987).
11) M. S. Carpenter, M. R. Melloch, M. S. Lundstrom, and S. P. Tobin, "Effects of Na_2S and $(NH_4)_2S$ edge passivation treatments on the dark current–voltage characteristics of GaAs pn diodes," Appl. Phys. Lett. **52**, 2157 (1988).
12) J-F. Fan, H. Oigawa, and Y. Nannichi, "The effect of $(NH_4)_2S$ treatment on the interface characteristics of GaAs MIS structures," Jpn. J. Appl. Phys. **27**, L1331 (1988).
13) D. M. Zhernokletov, H. Dong, B. Brennan, J. Kim, and R. M. Wallace, "Optimization of the ammonium sulfide $(NH_4)_2S$ passivation process on InSb(111)A," J. Vac. Sci. Technol. B **30**, 04E103 (2012).
14) D. Cuypers, D. H. van Dorp, M. Tallarida, S. Brizzi, L. Rodriguez, T. Conard, S. Arnauts, D. Schmeisser, C. Adelmann, and S. De Gendt, "Study of InP surfaces after wet chemical treatments," ECS J. Solid State Sci. Technol. **3**, N3016 (2014).
15) M. Oshima, T. Scimeca, Y. Watanabe, H. Oigawa, and Y. Nannichi, "Oxidation of sulfur-treated GaAs surfaces studied by photoluminescence and photoelectron spectroscopy," Jpn. J. Appl. Phys. **32**, 515 (1993).
16) Y. Nannichi, J-F. Fan, H. Oigawa, and A. Koma, "A model to explain the effective passivation of the GaAs surface by $(NH_4)_2S_x$ treatment," Jpn. J. Appl. Phys. **27**, L2367 (1988).
17) T. H. Yu, L. Yan, W. You, R. B. Laghumavarapu, D. Huffaker, and C. Ratsch, "The effect of passivation on different GaAs surfaces," Appl. Phys. Lett. **103**, 173902 (2013).
18) H. Xu, S. Belkouch, C. Aktik, and W. Rasmussen, "Se chemical passivation and annealing treatment for GaAs Schottky diode," Appl. Phys. Lett. **66**, 2125 (1995).
19) S. Tsukamoto and N. Koguchi, "Observation of sulfur-terminated GaAs (001)-(2×6) reconstruction by scanning tunneling microscopy," Appl. Phys. Lett. **65**, 2199 (1994).
20) M. J. Lowe, T. D. Veal, C. F. McCoville, G. R. Bell, S. Tsukamoto, and N. Koguchi, "Passivation and reconstruction-dependent electron accumulation at sulphur treated InAs(001) surfaces," Suf. Sci. **525**, 179 (2003).
21) S. A. Chambers and V. S. Sundaram, "Passivation of GaAs(001) surfaces by incorporation of group VI atoms: a structural investigation," J. Vac. Sci. Technol. B **9**, 2256 (1991).
22) S. Takatani, T. Kikawa, and M. Nakazawa, "Reflection high-energy electron-diffraction and photoemission spectroscopy study of GaAs(001) surface modified by Se adsorption," Phys. Rev. B **45**, 8498 (1992).
23) F. Maeda, Y. Watanabe, T. Scimeca, and M. Oshima, "Surface structure of Se-treated GaAs(001) from angle-resolved analysis of core-level photoelectron spectra," Phys. Rev. B **48**, 4956 (1993).
24) M. D. Pashley and D. Li, "Control of the Fermi-level position on the GaAs (001) surface: Se passivation," J. Vac. Sci. Technol. A **12**, 1848 (1994).
25) D. K. Biegelsen, R. D. Bringans, J. E. Northrup, and L-E. Swartz, "Selenium- and tellurium-terminated GaAs(100) surfaces observed by scanning tunneling microscopy," Phys. Rev. B **49**, 5424 (1994).
26) S. Takatani, A. Nakano, K. Ogata, and T. Kikawa, "Evidence of Ga_2Se_3-related compounds on Se-stabilized GaAs surfaces," Jpn. J. Appl. Phys. **31**, L458 (1992).
27) D. Li and M. D. Pashley, "Interaction of selenium with the GaAs(001)-(2×4)/c(2×8) surface studied by scanning tunneling microscopy," Phys. Rev. B **49**, 13643 (1994).
28) T. Scimeca, Y. Watanabe, R. Berrigan, and M. Oshima, "Surface chemical bonding of selenium-treated GaAs(111)A, (100), and (111)B," Phys. Rev. B **46**, 10201 (1992).
29) T. Scimeca, Y. Watanabe, F. Maeda, R. Berrigan, and M. Oshima, "Controlled passivation of GaAs by Se treatment," Appl. Phys. Lett. **62**, 1667 (1993).
30) S. Gundel and W. Faschinger, "First-principles simulation of Se and Te adsorbed on GaAs(001)," Phys. Rev. B **59**, 5602 (1999).
31) A. Ohtake, T. Suga, S. Goto, D. Nakagawa, and J. Nakamura, "Atomic structure of the Se-passivated GaAs(001) surface revisited," Sci. Rep. **13**, 18140 (2023).
32) A. Berthelot, I. Favero, G. Cassabois, C. Delalande, P. Rossignol, R. Ferreira, and J. M. Gérard, "Unconventional motional narrowing in the optical spectrum of a semiconductor quantum dot," Nat. Phys. **2**, 759 (2006).
33) M. Hauck, F. Seilmeier, S. E. Beavan, A. Badolato, P. M. Petroff, and A. Högele, "Locating environmental charge impurities with confluent laser spectroscopy of multiple quantum dots," Phys. Rev. B **90**, 235306 (2014).
34) N. Ha et al., "Size-dependent line broadening in the emission spectra of single GaAs quantum dots: impact of surface charge on spectral diffusion," Phys. Rev. B **92**, 075306 (2015).

35) S. Manna, H. Huang, S. F. C. da Silva, C. Schimpf, M. B. Rota, B. Lehner, M. Reindl, R. Trotta, and A. Rastelli, "Surface passivation and oxide encapsulation to improve optical properties of a single GaAs quantum dot close to the surface," Appl. Sur. Sci. **532**, 147360 (2020).
36) A. Chen, B-C. Juang, D. Ren, B. Liang, D. L. Prout, A. F. Chatziioannou, and D. L. Huffaker, "Significant suppression of surface leakage in GaSb/AlAsSb heterostructure with Al_2O_3 passivation," Jpn. J. Appl. Phys. **58**, 090907 (2019).
37) A. Higuera-Rodriguez, B. Romeira, S. Birindelli, L. E. Black, E. Smalbrugge, P. J. van Veldhoven, W. M. M. Kessels, M. K. Smit, and A. Fiore, "Ultralow surface recombination velocity in passivated InGaAs/InP nanopillars," Nano Lett. **17**, 2627 (2017).
38) D. Ren, K. M. Azizur-Rahman, Z. Rong, B-C. Juang, S. Somasundaram, M. Shahili, A. C. Farrell, B. S. Williams, and D. L. Huffaker, "Room-temperature midwavelength infrared InAsSb nanowire photodetector arrays with Al_2O_3 passivation," Nano Lett. **19**, 2793 (2019).
39) B. Jacob, F. Camarneiro, J. Borme, O. Bondarchuk, J. B. Nieder, and B. Romeira, "Surface passivation of III−V GaAs nanopillars by low-frequency plasma deposition of silicon nitride for active nanophotonic devices," ACS Appl. Electron. Mater. **4**, 3399 (2022).